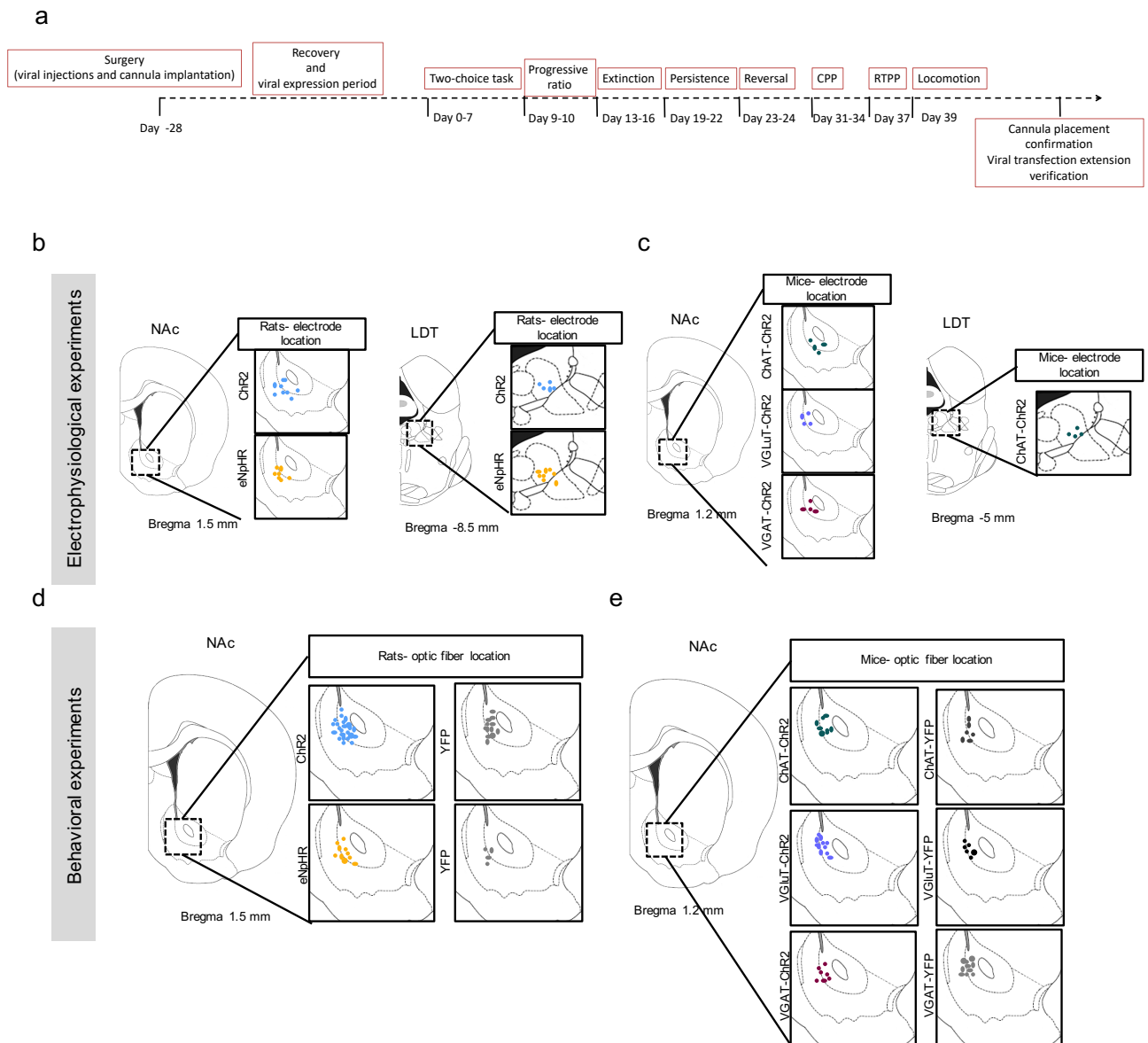


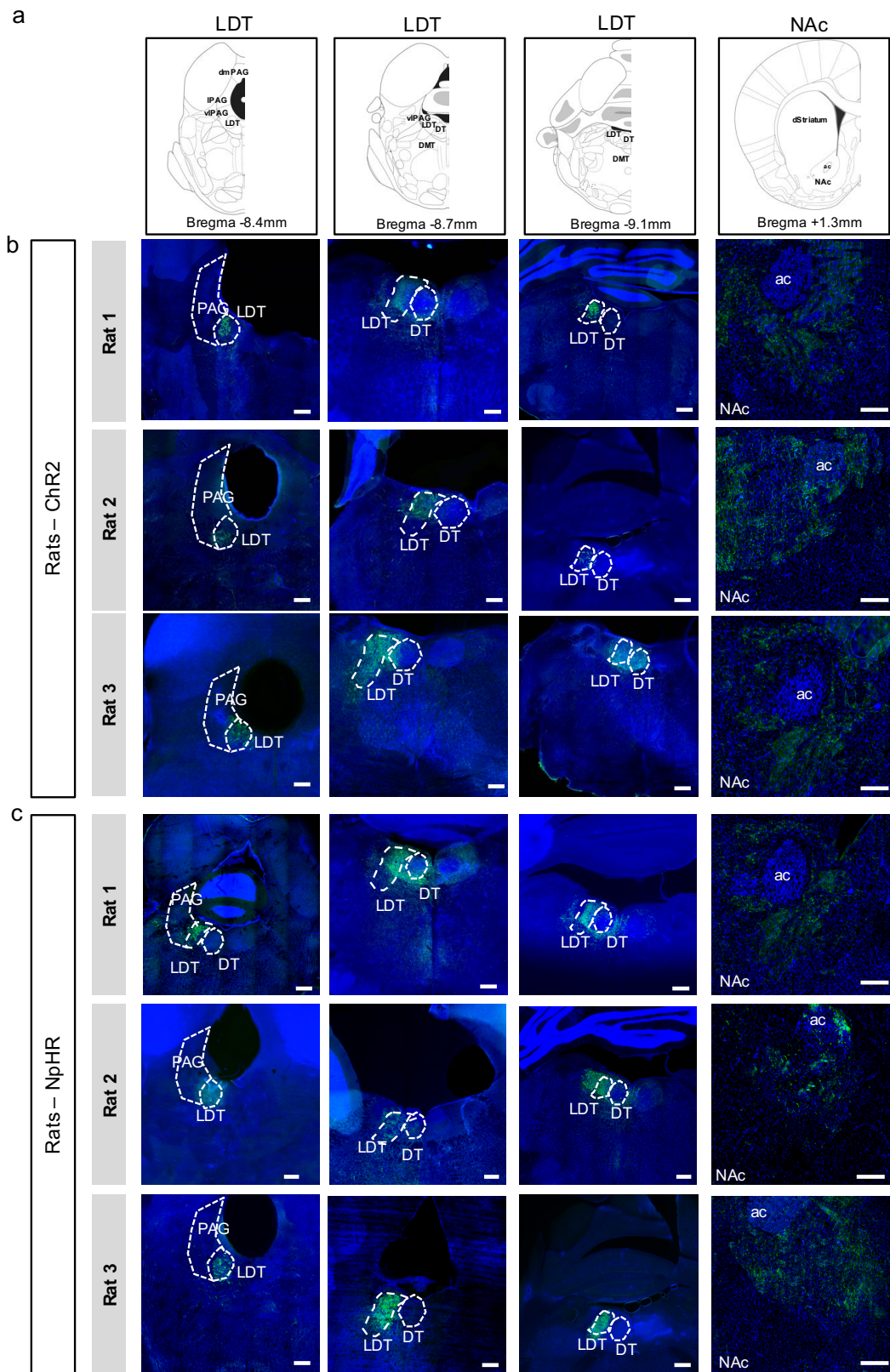
**Supplementary material – Coimbra B. *et al***

**Role of laterodorsal tegmentum projections to nucleus accumbens in reward-related behaviors**

Bárbara Coimbra, Carina Soares-Cunha, Nivaldo Vasconcelos, Ana Verónica Domingues, Sónia Borges, Nuno Sousa, Ana João Rodrigues

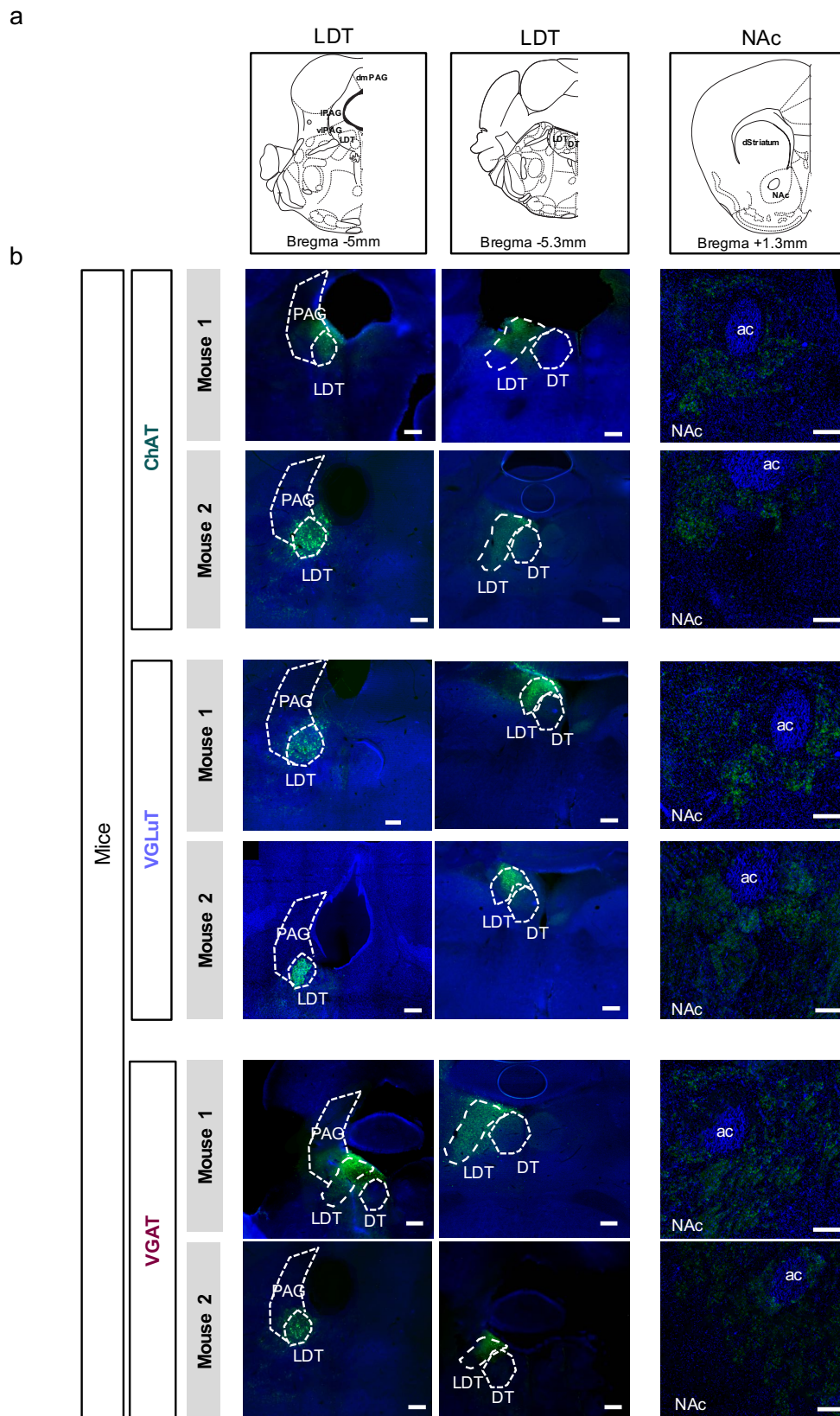


**Supplementary Figure 1.** Timeline of behavior and electrode and optic fiber placement confirmation. **(a)** Experimental timeline of experiments. **(b-c)** Electrode placement of animals used for electrophysiological experiments: **(b)** rats and **(c)** mice. Schematic representation of optic fiber placement in LDT terminals in the NAc of **(d)** rats and **(e)** mice that performed behavioral experiments.



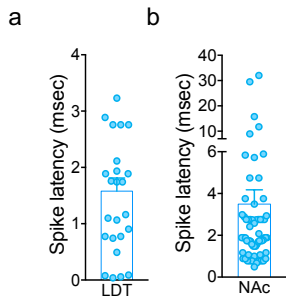
**Supplementary Figure 2.** Confirmation of viral expression in rats. **(a)** Schematic representation of LDT and NAc coordinates of brain sections depicted in b-c. **(b-c)** Immunofluorescence showing YFP staining in the LDT region of 3 representative animals of ChR2 and NpHR groups; 3 different sections are shown. In the right, it is also depicted one section of the NAc showing the presence of YFP<sup>+</sup> terminals.

Scale bars from LDT slices=1 mm; scale bars from NAc slice =500  $\mu$ m PAG: periaqueductal gray; DT: dorsal tegmental nucleus.

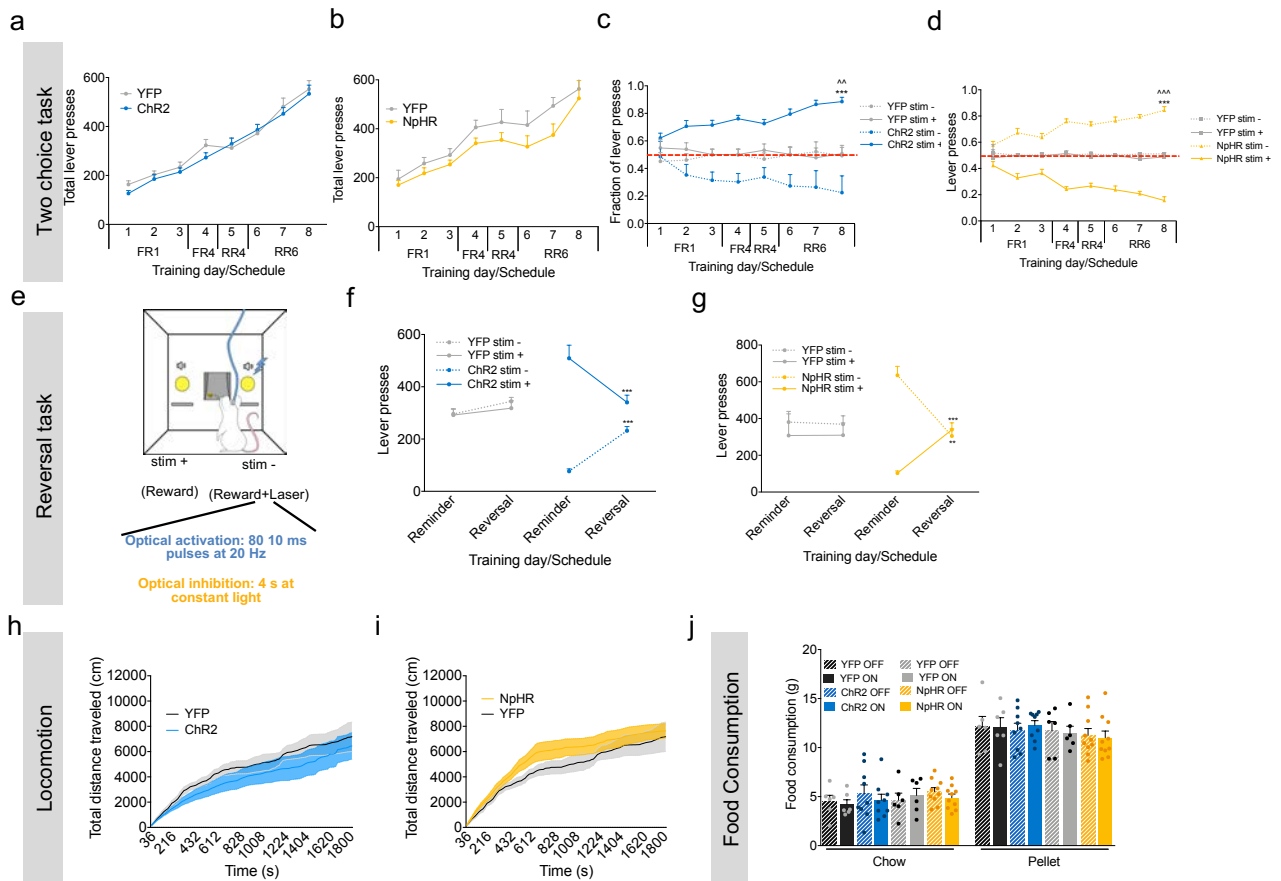


**Supplementary Figure 3.** Confirmation of viral expression in mice. **(a)** Schematic representation of LDT and NAc coordinates of brain sections depicted in **b**. **(b)** Immunofluorescence showing YFP staining in the LDT and LDT terminals in the NAc of 2 representative animals of ChAT, VGLuT and VGAT groups.

Scale bars from LDT slices =1 mm; scale bars from NAc slice =500  $\mu$ m; PAG: periaqueductal gray; DT: dorsal tegmental nucleus.

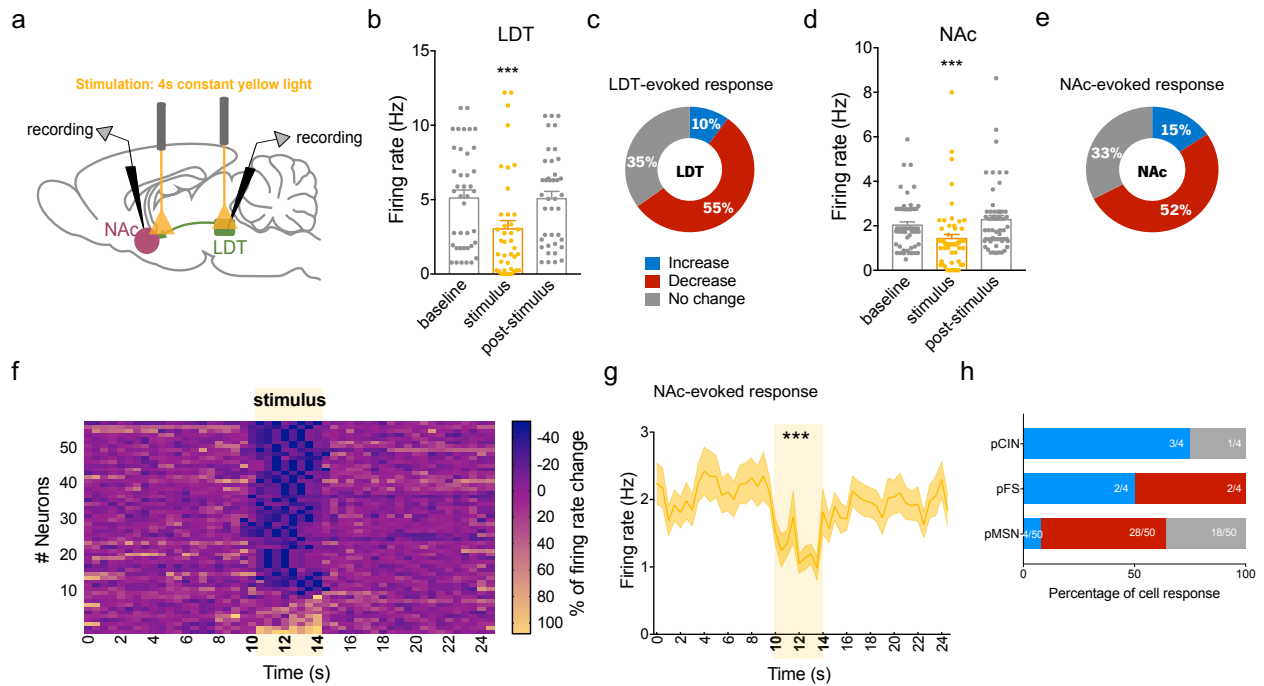


**Supplementary Figure 4.** Spike latency to optical stimulation. **(a)** Latency of LDT neurons response to soma optical stimulation (80 10ms pulses at 20 Hz). **(b)** Latency of response of NAc neurons to LDT terminal optical stimulation (80 10ms pulses at 20 Hz).



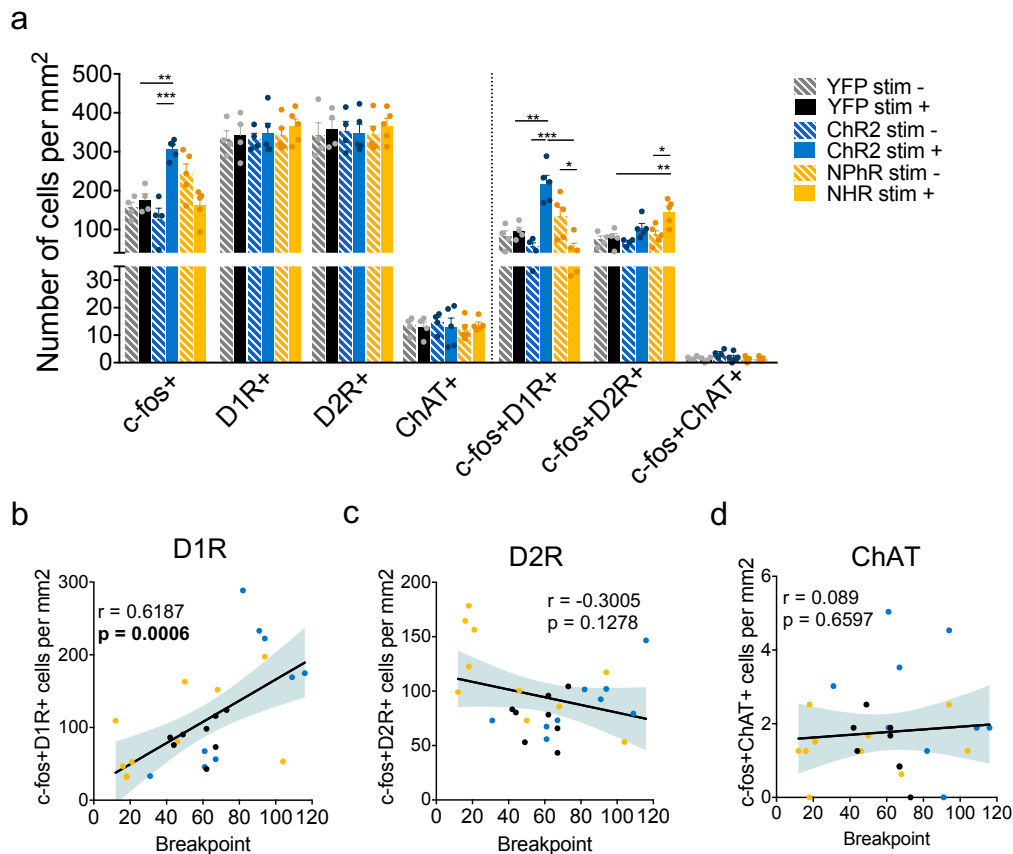
**Supplementary Figure 5.** Optogenetic modulation of LDT-NAc terminals does not affect behavioral flexibility, food consumption or locomotion. Total number of lever presses in the two-choice task of (a) ChR2 and (b) NpHR animals are similar to YFP animals. Fraction of lever presses for each session during the two-choice task of (c) ChR2 and (d) NpHR animals. (e) Two-choice task representation of reversal session. (f) Reversal session of ChR2 and respective YFP control animals. Stim- was switched for stim+ and vice versa. ChR2 animals shift preference for the new stim+ lever, showing behavioral flexibility. (g) Reversal session of NpHR and respective YFP control animals. Stim- was switched for stim+ and vice versa. NpHR animals shift preference for the new stim- lever, showing behavioral flexibility. (h-i) No impact in locomotion by optical activation or inhibition of LDT-NAc projections. (j) No differences in food consumption of chow or palatable food by optical activation or inhibition of LDT-NAc projections.

Values are shown as mean  $\pm$  s.e.m. \*refers to difference between ChR2/NpHR stim+ and stim- lever; RM 2way ANOVA. ^refers to difference between ChR2/NpHR stim+ and YFP stim+ lever; RM 2way ANOVA. \*\* $p < 0.01$ , \*\*\* $p < 0.001$ .



**Supplementary Figure 6.** LDT-NAc terminal optical inhibition decreases NAc electrophysiological activity. **(a)** Strategy used for optogenetic inhibition and electrophysiological recordings. An AAV-WGA-cre fusion vector was injected unilaterally in the NAc and a cre-dependent NpHR in the LDT. **(b)** During optical inhibition (4s of constant yellow light at 10mW) of LDT cell bodies, LDT decreases firing rate ( $n=8$  animals; 40 LDT cells; RM 1way ANOVA). **(c)** 55% of LDT recorded cells decreased their firing rate during inhibition while no change was detected in 35% of cells; 10% increased the firing rate. **(d)** Firing rate in the NAc is decreased during optical inhibition of LDT terminals ( $n=7$  animals; 58 cells; RM 1way ANOVA). **(e)** Around half of recorded cells in the NAc showed decreased the firing rate upon stimulation, 33% presented no change and 15% increased activity. **(f)** Heatmap representation of cell responses in the NAc to stimulation of LDT terminals with yellow laser. **(g)** Average firing rate of NAc neurons showing a decrease from the baseline during stimulation of LDT-NAc inputs (KS test). **(h)** During LDT terminal inhibition, 56% of recorded MSNs decreased their activity (28/50 cells), 36% did not change firing rate (18/50 cells) and 8% increased their activity (4/50 cells); 75% pCINs (3/4 cells) and 50% pFS (2/4 cells) interneurons increased, 25% pCINs (1/4 cells) did not change and 50% pFS (2/4 cells) interneurons decreased their activity.

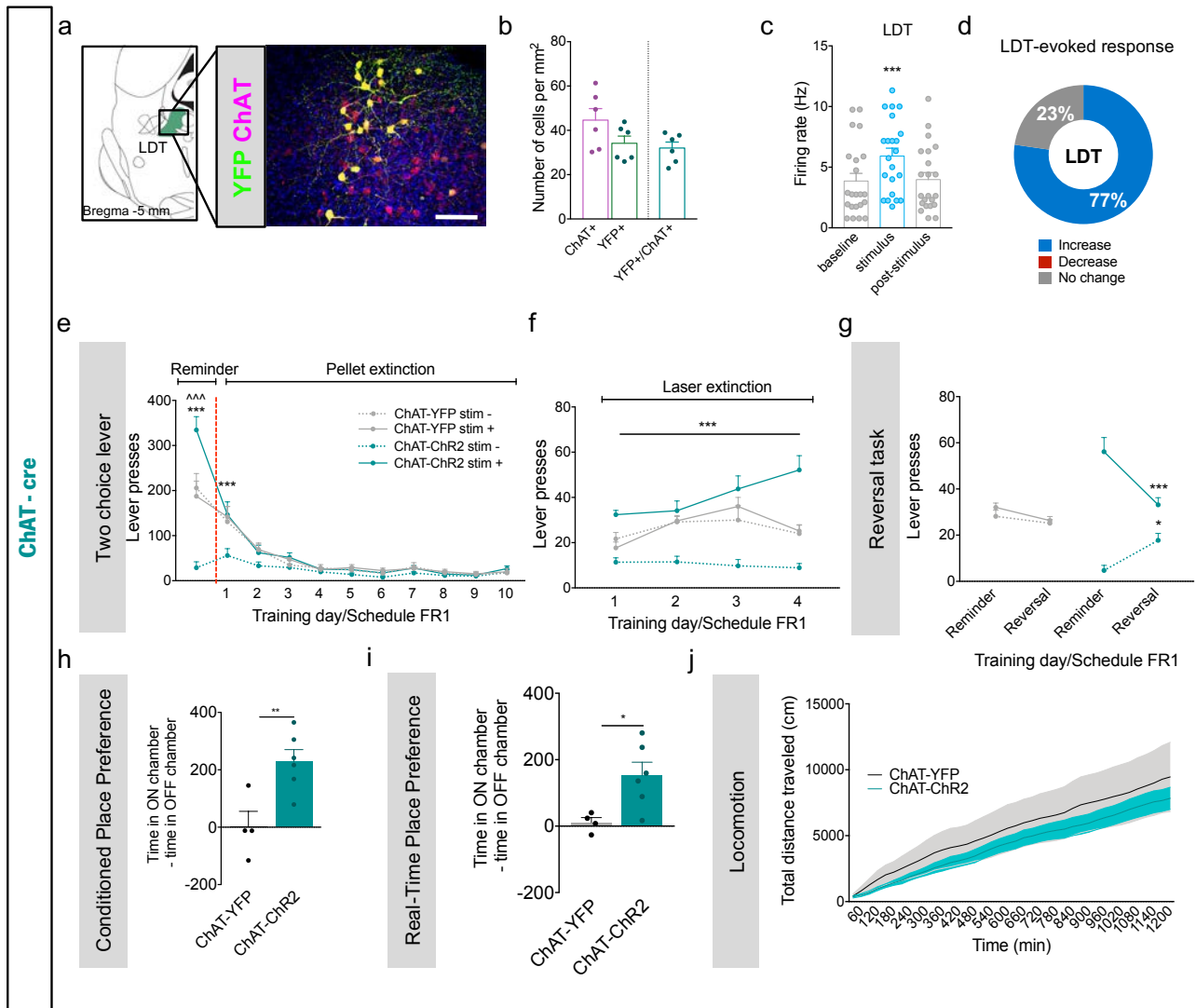
Values are shown as mean  $\pm$  s.e.m. \*\*\* $p<0.001$ .



**Supplementary Figure 7.** Optical activation of LDT-NAc terminals mainly recruits NAc D1-MSNs. **(a)** Quantification of c-fos and D1R, DR2 or ChAT double positive cells in ChR2 ( $n_{stim+}=5$ ;  $n_{stim-}=4$ ), NpHR ( $n_{stim+}=5$ ;  $n_{stim-}=5$ ) and YFP ( $n_{stim+}=4$ ;  $n_{stim-}=4$ ) rats after PR performance on the stim+ or stim- lever. There is a substantial increase in the number of c-fos<sup>+</sup>/D1R<sup>+</sup> cells after LDT-NAc optical activation, whereas optical inhibition appears to recruit mostly D2R cells. No significant differences were found in the number of c-fos<sup>+</sup>/ChAT<sup>+</sup> cells (1 way ANOVA). **(b)** Pearson's correlation between individual breakpoint of ChR2, NpHR or YFP animals and the number of c-fos<sup>+</sup>/D1<sup>+</sup> cells in the NAc. There is a positive correlation between the number of D1R recruited cells in the NAc and individual motivational drive (given by the breakpoint in the PR task). **(c)** Pearson's correlation between individual breakpoint and the number of c-fos<sup>+</sup>/D2<sup>+</sup> cells. No significant differences were found. **(d)** Pearson's correlation between individual breakpoint and the number of c-fos<sup>+</sup>/ChAT<sup>+</sup> cells. No significant differences were found.

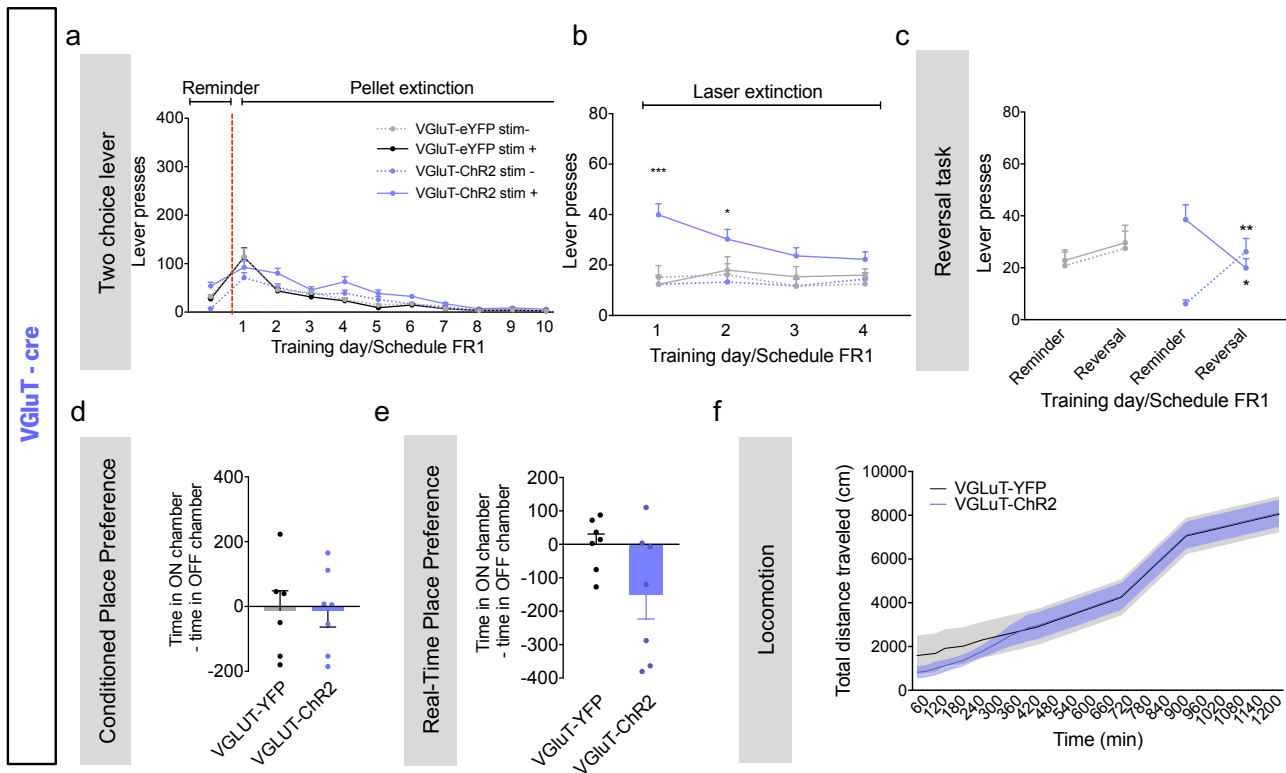
Values are shown as mean  $\pm$  s.e.m. \* $p < 0.05$ ; \*\* $p < 0.01$ ; \*\*\* $p < 0.001$ .





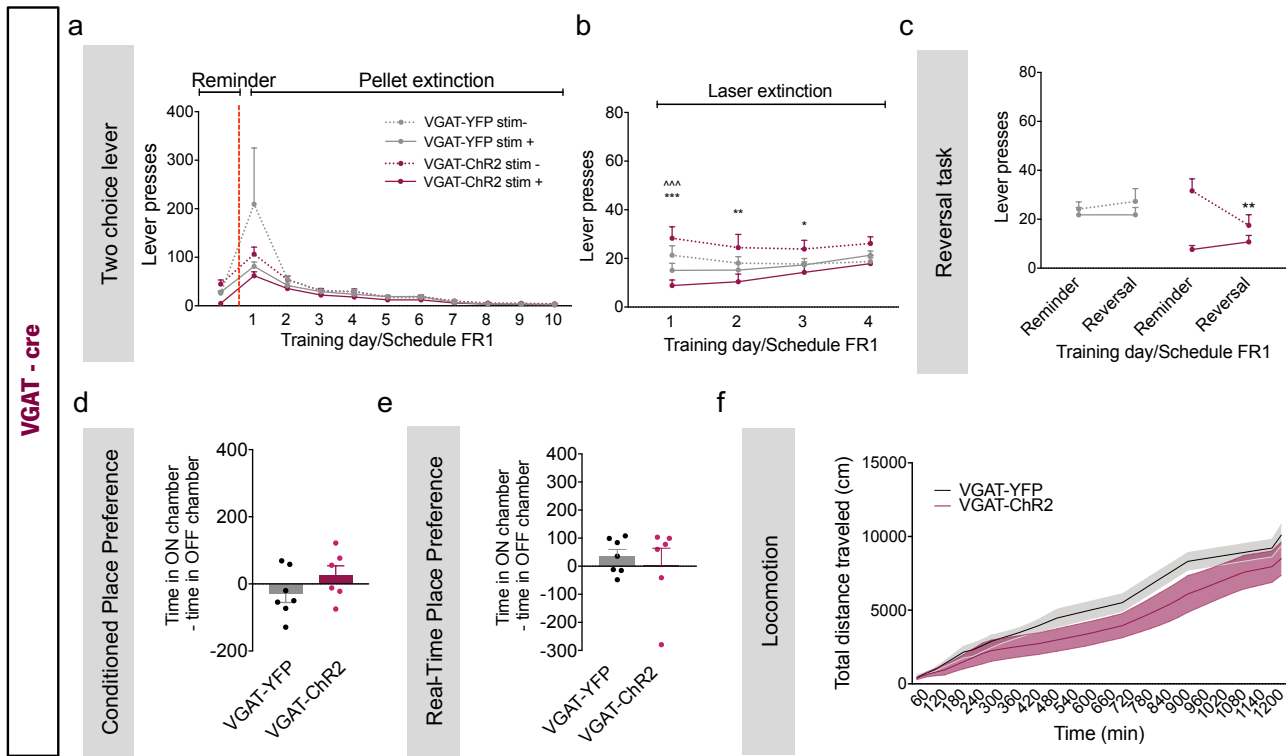
**Supplementary Figure 8.** Behavioral effects of optical activation of LDT-NAc cholinergic terminals. **(a)** Representative immunofluorescence for YFP and ChAT; scale bar=100  $\mu$ m. **(b)** Respective quantification of double positive cells (n=6 animals). **(c)** LDT neurons increase firing rate in response to optical activation of LDT cell bodies (stimulation: 80 10 ms pulses at 20 Hz) (n=4 animals; 22 cells; RM 1way ANOVA). **(d)** 77% of LDT recorded cells increased their firing rate to optical stimulation. **(e)** In pellet extinction conditions, ChAT-ChR2 and ChAT-YFP groups decrease responses for stim+ and stim- levers, despite pressing stim+ still originates LDT-NAc cholinergic terminals stimulation. **(f)** In laser extinction conditions, ChAT-ChR2 animals still manifest preference for the stim+ lever, despite no stimulation is given; ChAT-YFP animals do not manifest preference. **(g)** ChAT-ChR2 animals shift their preference for the new stim+ lever in a reversal task. \*refers to difference between ChAT-ChR2 stim+ and stim- lever, RM 2way ANOVA; ^refers to difference between ChAT-ChR2 stim+ and ChAT-YFP stim+ lever, RM 2way ANOVA. Difference between time spent in the ON and OFF chambers in the **(h)** CPP and **(i)** RTPP, showing preference for the ON chamber in both tests (t test). **(j)** No significant impact in locomotion by optical activation of LDT-NAc cholinergic projections (n<sub>ChAT-ChR2</sub>=6, 2 animals lost cannula; n<sub>ChAT-YFP</sub>=4, 2 animals lost cannula).

Values are shown as mean  $\pm$  s.e.m. \*p<0.05; \*\*p<0.01; \*\*\*p<0.001.

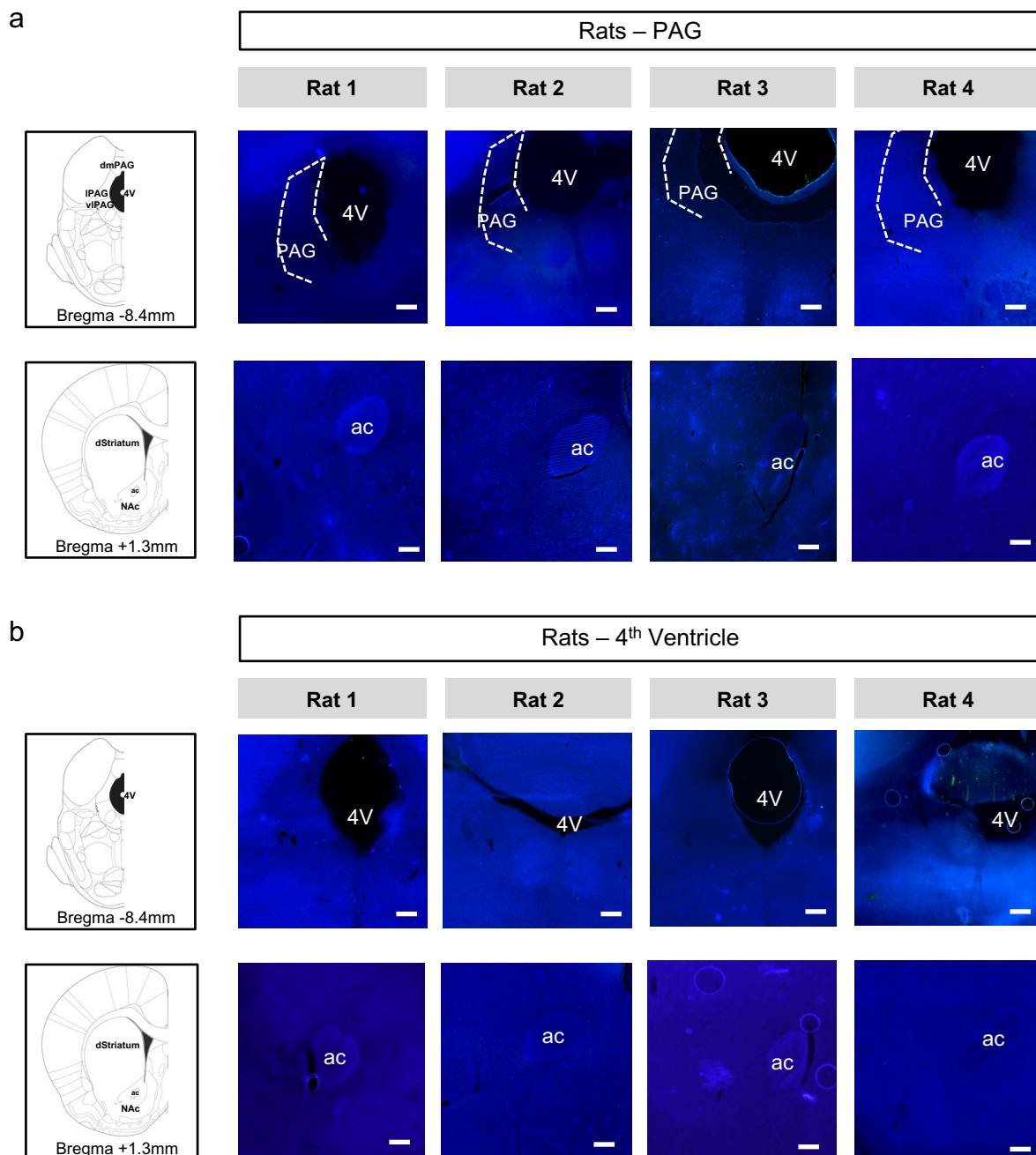


**Supplementary Figure 9.** Behavioral effects of optical activation of LDT-NAc glutamatergic terminals. **(a)** During pellet extinction conditions, VGLuT-ChR2 and VGLuT-YFP animals decreased lever pressing for both levers. **(b)** VGLuT-ChR2 animals retain preference for stim+ lever in laser extinction conditions for the first 2 sessions, though they decrease the number of presses throughout sessions. **(c)** VGLuT-ChR2 animals shift their preference for the new stim+ lever in a reversal task. **(d)** Difference between time spent in the ON and OFF chambers, showing no differences between groups. **(e)** Difference between time spent in the ON and OFF chambers in the RTPP. **(f)** No impact in locomotion by optical activation of LDT-NAc glutamatergic projections.

Values are shown as mean  $\pm$  s.e.m. \*refers to difference between VGLuT-ChR2 stim+ and stim- lever, RM 2way ANOVA. \* $p < 0.05$ ; \*\* $p < 0.01$ ; \*\*\* $p < 0.001$ .

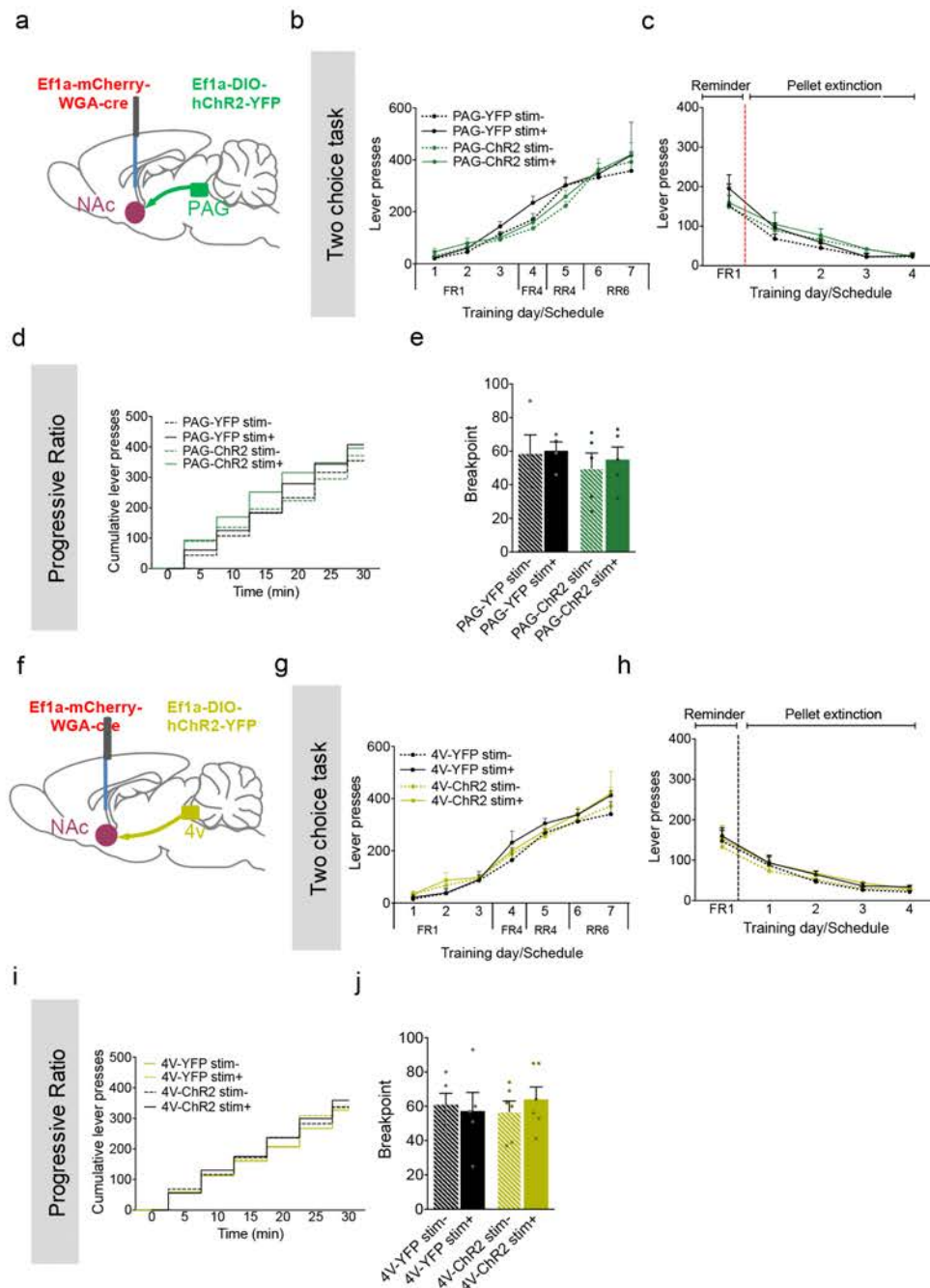


**Supplementary Figure 10.** Behavioral effects of optical activation of LDT-NAc GABAergic terminals. **(a)** In pellet extinction conditions, VGAT-ChR2 and VGAT-YFP have reduced number of presses in both levers. **(b)** In laser extinction conditions, VGAT-ChR2 animals still retain preference for the stim- lever. **(c)** VGAT-ChR2 animals decrease their preference for the new stim+ lever in a reversal task. **(d)** Difference between time spent in the ON and OFF chambers in the CPP test, showing no differences between groups. **(e)** Difference between time spent in the ON and OFF chambers in the RTPP. **(f)** No impact in locomotion by optical activation of LDT-NAc GABAergic projections ( $n_{\text{VGAT-ChR2}}=6$ , 1 animal lost cannula;  $n_{\text{VGAT-YFP}}=7$ , 4 animals lost cannula). Values are shown as mean  $\pm$  s.e.m. \*refers to difference between VGAT-ChR2 stim+ and stim- lever, RM 2way ANOVA; ^refers to difference between VGAT-ChR2 stim+ and VGAT-YFP stim+ lever, RM 2way ANOVA. \* $p<0.05$ ; \*\* $p<0.01$ ; \*\*\* $p<0.001$



**Supplementary Figure 11.** Histological evaluation of control groups injected in the periaqueductal grey (PAG) and 4<sup>th</sup> ventricle (4V). (a) One group of animals was injected with WGA-cre in NAc + DIO-ChR2 in the PAG. No YFP expression was found in the PAG nor in the NAc. (b) Another group of animals was injected with WGA-cre in NAc + DIO-ChR2 in the 4<sup>th</sup> Ventricle. No expression of YFP+ cells in the 4<sup>th</sup> Ventricle nor adjacent areas, nor YFP+ terminals in the NAc was found.

Scale bars = 0.5 mm.



**Supplementary Figure 12.** Behavioral evaluation of control groups, in which PAG-NAc or 4<sup>th</sup>V-NAc “terminals” were stimulated (vide also Sup. Fig. 11, showing the absence of staining, indicative of the lack of projections of either region). **(a)** Strategy used in order to stimulate PAG hypothetical terminals in the NAc. One group of animals was injected with WGA-cre in NAc + DIO-ChR2 in the PAG, and optically stimulated in the NAc. **(b)** Stimulation of hypothetical PAG terminals in the NAc did not induce any preference in the two-choice task. **(c)** All groups decrease responding in pellet extinction conditions. **(d-e)** No effect of “PAG-NAc terminals” optogenetic activation in the progressive ratio test ( $n_{\text{PAG-ChR2}}=5$ ,  $n_{\text{PAG-YFP}}=4$ ). **(f)** Strategy used to control for misplaced injection in the 4V. One group of animals was injected with WGA-cre in NAc + DIO-ChR2 in the 4V. **(g)** Stimulation of hypothetical terminals in the NAc did not induce any preference in the two-choice task. **(h)** All groups decrease responding in pellet extinction conditions. **(i-j)** No effect of optogenetic activation in the progressive ratio test ( $n_{4\text{V-ChR2}}=6$ ,  $n_{4\text{V-YFP}}=5$ ).

Values are shown as mean  $\pm$  s.e.m.